

Thermodynamics of the one-dimensional frustrated Heisenberg ferromagnet with arbitrary spin

M. Härtel and J. Richter

Institut für Theoretische Physik, Otto-von-Guericke-Universität Magdeburg, D-39016 Magdeburg, Germany

D. Ihle

Institut für Theoretische Physik, Universität Leipzig, D-04109 Leipzig, Germany

J. Schnack

Universität Bielefeld, Fakultät für Physik, Postfach 100131, D-33501 Bielefeld, Germany

S.-L. Drechsler

Leibniz-Institut für Festkörper- und Werkstoffforschung Dresden, D-01171 Dresden, Germany

(Dated: June 7, 2011)

The thermodynamic quantities (spin-spin correlation functions $\langle \mathbf{S}_0 \mathbf{S}_n \rangle$, correlation length ξ , spin susceptibility χ , and specific heat C_V) of the frustrated one-dimensional J_1 - J_2 Heisenberg ferromagnet with arbitrary spin quantum number S below the quantum critical point, i.e. for $J_2 < |J_1|/4$, are calculated using a rotation-invariant Green-function formalism and full diagonalization as well as a finite-temperature Lanczos technique for finite chains of up to $N = 18$ sites. The low-temperature behavior of the susceptibility χ and the correlation length ξ is well described by $\chi = \frac{2}{3}S^4 (|J_1| - 4J_2) T^{-2} + AS^{5/2} (|J_1| - 4J_2)^{1/2} T^{-3/2}$ and $\xi = S^2 (|J_1| - 4J_2) T^{-1} + BS^{1/2} (|J_1| - 4J_2)^{1/2} T^{-1/2}$ with $A \approx 1.1 \dots 1.2$ and $B \approx 0.84 \dots 0.89$. The vanishing of the factors in front of the temperature at $J_2 = |J_1|/4$ indicates a change of the critical behavior of χ and ξ at $T \rightarrow 0$. The specific heat may exhibit an additional frustration-induced low-temperature maximum when approaching the quantum critical point. This maximum appears for $S = 1/2$ and $S = 1$, but was not found for $S > 1$.

PACS numbers:

I. INTRODUCTION

The one-dimensional (1D) Heisenberg model with ferromagnetic nearest-neighbor (NN) exchange $J_1 < 0$ and frustrating antiferromagnetic next nearest-neighbor (NN) exchange $J_2 \geq 0$ has recently attracted much attention, see, e.g., Refs. 1–12. This model may serve as the minimal model to describe the physical properties of edge-shared chain cuprates, e.g. $\text{Ca}_2\text{Y}_2\text{Cu}_5\text{O}_{10}$, $\text{Li}_2\text{ZrCuO}_4$, and Li_2CuO_2 .^{12–15} On the other hand, several materials considered as 1D ferromagnets, such as $\text{TMCuC}[(\text{CH}_3)_4\text{NCuCl}_3]$,¹⁶ CsNiF_3 ,¹⁷ $\text{Ni}(\text{4-cyanopyridine})_2\text{Cl}_2$ ¹⁸ or deposited Co chains¹⁹ might have also a weak frustrating NNN exchange $J_2 < -J_1/4$. Moreover, recent investigations suggest that Li_2CuO_2 as well as $\text{Ca}_2\text{Y}_2\text{Cu}_5\text{O}_{10}$ are quasi-1D spin systems with a dominant ferromagnetic J_1 and weak frustrating antiferromagnetic J_2 so that the inchain spin-spin correlations are predominantly ferromagnetic.^{12,13,15}

The corresponding Hamiltonian of the 1D J_1 - J_2 Heisenberg model considered in this paper is given by

$$H = \sum_i (J_1 \mathbf{S}_i \mathbf{S}_{i+1} + J_2 \mathbf{S}_i \mathbf{S}_{i+2}), \quad (1)$$

where i runs over all lattice sites and $\mathbf{S}_i^2 = S(S+1)$. We set $J_1 = -1$ and consider $J_2 \geq 0$. Although some of the above mentioned materials, namely CsNiF_3 ,¹⁷ $\text{Ni}(\text{4-cyanopyridine})_2\text{Cl}_2$ ¹⁸ or deposited Co chains¹⁹, represent

1D ferromagnets with spin quantum number $S > 1/2$, so far the focus of recent theoretical studies has been on the $S = 1/2$ case. Since Haldane's famous paper²⁰ we know that in 1D Heisenberg systems the spin quantum number may play a crucial role. Recently it has been found that the frustrated model (1) in the extreme quantum case $S = 1/2$ may exhibit a different behavior near the quantum critical point than the model for $S > 1/2$.⁴ Moreover, in Ref. 21 it has been found that for the unfrustrated 1D quantum ferromagnets a characteristic field-induced low-temperature maximum in the specific heat exists only for the small spin quantum numbers $S = 1/2$ and $S = 1$, see also Refs. 11,22,23.

In the present paper we discuss the thermodynamics of the model (1) for arbitrary spin quantum number S and focus on the parameter regime $J_2 < |J_1|/4$, where the ferromagnetic ground state is realized. It has been recently demonstrated for low-dimensional frustrated ferromagnets,^{7,11,24,25} that the frustrating J_2 may influence the thermodynamics substantially. In the 1D system a change in the low-temperature behavior of the susceptibility and the correlation length as well as an additional low-temperature maximum in the specific heat have been found when approaching the zero-temperature critical point at $J_2 = |J_1|/4$ from the ferromagnetic side.⁷ In particular, a different critical behavior of the susceptibility and the correlation length has been found for $J_2 < |J_1|/4$ and at $J_2 = |J_1|/4$.^{7,25}

As in our previous papers on frustrated spin-1/2 ferromagnets,^{7,11,24} we use a second-order Green-function technique²⁶ to study the influence of the spin quantum number S on the thermodynamic properties of the model (1). This technique has been applied successfully to several low-dimensional quantum spin systems.^{7,11,21–24,26–30}

To extend our Green's function theory⁷ to $S > 1/2$, we follow Ref. 30, where the Green's function technique was applied to a ferro- and antiferromagnetic layered square lattice with arbitrary S . We complement the Green's function results by full exact diagonalization (ED) and finite-temperature Lanczos (FTL) technique data for finite systems of up to $N = 18$ lattice sites.

II. FULL DIAGONALIZATION AND FINITE-TEMPERATURE LANCZOS TECHNIQUE FOR FINITE LATTICES

Using Schulenburg's *spinpack*³¹ and exploiting the lattice symmetries and the fact that $S^z = \sum_i S_i^z$ commutes with H we are able to calculate the exact thermodynamics for periodic chains of up to $N = 14$ spins for spin quantum number $S = 1$. For $N = 8$ sites we found the exact thermodynamics up to $S = 2$. Clearly, the full ED of finite systems for $S > 1/2$ is less efficient as for $S = 1/2$, since the accessible system size N decreases with increasing of S .

In addition to the full ED we have also applied a FTL technique, see e.g. Refs. 33,34. This method allows an accurate calculation of thermodynamic quantities down to low temperatures for $S = 1$ up to $N = 18$.

III. SPIN-ROTATION-INVARIANT GREEN-FUNCTION THEORY

To study the thermodynamics of the model (1) for arbitrary N we use the spin-rotation-invariant Green-function method (RGM).^{7,24,26–28,30} The relevant thermodynamic quantities can be determined by calculating the two-time commutator Green function³² $\langle\langle S_q^+; S_{-q}^- \rangle\rangle_\omega$, which is related to the transverse spin susceptibility by $\chi_q^{+-}(\omega) = -\langle\langle S_q^+; S_{-q}^- \rangle\rangle_\omega$. Using the equations of motion up to the second step and supposing rotational symmetry with $\langle S_i^z \rangle = 0$, we obtain $\omega^2 \langle\langle S_q^+; S_{-q}^- \rangle\rangle_\omega = M_q + \langle\langle -\ddot{S}_q^+; S_{-q}^- \rangle\rangle_\omega$ with $M_q = \langle\langle [S_q^+, H], S_{-q}^- \rangle\rangle$ and $-\ddot{S}_q^+ = \langle\langle [S_q^+, H], H \rangle\rangle$. For the moment M_q the exact expression

$$M_q = -4 \sum_{n=1,2} J_n C_n (1 - \cos nq) \quad (2)$$

holds, where $C_n = \langle S_0^+ S_n^- \rangle = 2 \langle S_0^z S_n^z \rangle$. The second derivative $-\ddot{S}_q^+$ is approximated in the spirit of Refs. 21–24,26–30, i.e., in $-\ddot{S}_q^+$ we use the decoupling $S_i^+ S_j^+ S_k^- = \alpha \langle S_j^+ S_k^- \rangle S_i^+ + \alpha \langle S_i^+ S_k^- \rangle S_j^+$, and $S_i^+ S_j^- S_j^+ =$

$\langle S_j^- S_j^+ \rangle S_i^+ + \lambda \langle S_i^+ S_j^- \rangle S_j^+$ for products with two coinciding sites which occur for $S \geq 1$.^{21,27,29,30} Note that for $J_2 < -J_1/4$, where the ground-state is ferromagnetic, the vertex parameters α and λ can be assumed in a good approximation to be independent of the range of the associated spin correlators, cf. Ref. 7. Then we obtain $-\ddot{S}_q^+ = \omega_q^2 S_q^+$ and

$$\chi_q^{+-}(\omega) = -\langle\langle S_q^+; S_{-q}^- \rangle\rangle_\omega = \frac{M_q}{\omega_q^2 - \omega^2}, \quad (3)$$

with

$$\omega_q^2 = \sum_{n,m=(1,2)} J_n J_m (1 - \cos nq) [K_{n,m} + 4\alpha C_n (1 - \cos mq)], \quad (4)$$

where $K_{n,n} = \frac{4}{3}S(S+1) + 2\lambda C_n + 2\alpha(C_{2n} - 3C_n)$, $K_{1,2} = 2\alpha(C_3 - C_1)$, and $K_{2,1} = K_{1,2} + 4\alpha(C_1 - C_2)$. From the Green function (3) the correlation functions $C_n = \frac{1}{N} \sum_q C_q e^{iqn}$ are determined by the spectral theorem,³²

$$C_q = \langle S_q^+ S_{-q}^- \rangle = \frac{M_q}{2\omega_q} [1 + 2n(\omega_q)], \quad (5)$$

where $n(\omega_q) = (e^{\omega_q/T} - 1)^{-1}$ is the Bose function. Using the operator identity $\mathbf{S}_i^2 = S_i^+ S_i^- - S_i^z + (S_i^z)^2$, we get the sum rule $C_0 = \frac{1}{N} \sum_q C_q = \frac{2}{3}S(S+1)$. Following Ref. 30, as an additional equation to determine the vertex parameters we consider the ratio

$$r(T) = \frac{\lambda(T) - \lambda(\infty)}{\alpha(T) - \alpha(\infty)} = r(0) \quad (6)$$

as temperature independent, where $\lambda(\infty) = 1 - \frac{3}{4S(S+1)}$ and $\alpha(\infty) = 1$, see Ref. 29. The uniform static spin susceptibility $\chi = \lim_{q \rightarrow 0} \chi_q$, where $\chi_q = \chi_q(\omega = 0)$ and $\chi_q(\omega) = \frac{1}{2} \chi_q^{+-}(\omega)$, is given by

$$\chi = -\frac{2}{\Delta} \sum_{n=1,2} n^2 J_n C_n; \quad \Delta = \sum_{n,m=(1,2)} n^2 J_n J_m K_{n,m}. \quad (7)$$

The correlation length ξ for a ferromagnet can be calculated from the expansion of the static spin susceptibility around $q = 0$ (see, e.g., Refs. 26 and 21), $\chi_q = \chi / (1 + \xi^2 q^2)$. The ferromagnetic long-range order, occurring in the 1D model at zero temperature only, is related to the condensation term C (see Ref. 26) via $C_n(0) = \frac{1}{N} \sum_{q(\neq 0)} (M_q/2\omega_q) e^{iqn} + C$. Equating this expression to the exact result $C_n(0) = \frac{2}{3}S\delta_{n,0} + \frac{2}{3}S^2$ leads to $C(0) = \frac{2}{3}S^2$ and $M_q(0)/2\omega_q(0) = \frac{2}{3}S$.³⁰ This requires $\alpha(0) = \frac{3}{2}$ and $K_{n,m}(0) = 0$ [cf. Eqs. (2) and (4)] which leads to $\lambda(0) = 2 - \frac{1}{S}$. The parameter Δ in Eq. (7) is zero at $T = 0$, i.e., χ diverges as $T \rightarrow 0$ according to the ferromagnetic phase transition. Moreover, using these results we find at zero temperature $\omega_q = 2\rho_s q^2$ ($|q| \ll 1$), $\rho_s = \frac{S}{2}(|J_1| - 4J_2)$, where ρ_s is the spin stiffness.

Since we will compare the RGM data with ED data for finite lattices, see Sec. IV, we have to adopt the RGM to finite N . In this case the quantity C is not related to the magnetisation and stays nonzero in the whole temperature region. In Ref. 29 it was shown that $C = 2T\chi/N$.

Finally, to solve the equation of motion and to evaluate the thermodynamic quantities we have to determine the correlators C_l ($l = 1, \dots, 4$) and the vertex parameters α and λ (for finite systems, also C) as the numerical solution of a coupled system of six (seven) non-linear algebraic self-consistency equations: C_l according to Eq. (5) including the sum rule $C_0 = \frac{1}{2}$, and the ratio Eq. (6). To find the numerical solution of the RGM equations for $T > 0$, we start at high temperatures and decrease T in small steps. Below a certain (low) temperature $T_0(J_2, S)$ no solutions of the RGM equations (except at $T = 0$) could be found, since the quantity $\Delta(T, J_2, S)$ in Eq. (7) becomes exponentially small which leads to numerical uncertainties. We find that $T_0(J_2, S)/S(S+1)$ is of the order of 10^{-3} for all values of J_2 and S considered here. Moreover, we find that the RGM solution at very low temperatures becomes less trustworthy for J_2 approaching the quantum critical point $J_2 = |J_1|/4$, cf. also Refs. 7 and 11. Therefore, below we will present RGM results for $J_2 \leq 0.22|J_1|$ only.

IV. RESULTS

Motivated by the high-temperature behavior of the physical quantities^{37,38} we use as the renormalized temperature scale $t = T/S(S+1)$, since for large temperatures physical quantities exhibit t -dependence which is independent of S .

A. Spin-spin correlation functions

Let us first consider the spin-spin correlation functions $\langle \mathbf{S}_0 \mathbf{S}_n \rangle$ depicted in Fig. 1 for NN, NNN and tenth-nearest neighbors. Analogously to the frustrated $S = 1/2$ chain,⁷ with increasing frustration the correlation functions decrease more rapidly. Obviously the spin quantum number S has only a small influence on the correlation functions as functions of t . Interestingly, an increase of S yields a slight weakening of the short-range spin-spin correlation at fixed $t > 0$ (see upper and middle panels in Fig. 1), but an enhancement of larger-distant correlations (see lower panel in Fig. 1). Moreover, the NNN correlation function for $J_2 = 0.2$ becomes negative at $t = t_0 \approx 1.35, 1.37, 1.38$ for $S = 1, 3/2, 2$, respectively. (Note that for $S = 1/2$ the corresponding temperature is $t_0 \approx 1.27$.)

B. Susceptibility and correlation length

The behavior of the correlation functions is reflected in the susceptibility χ and the correlation length ξ shown in

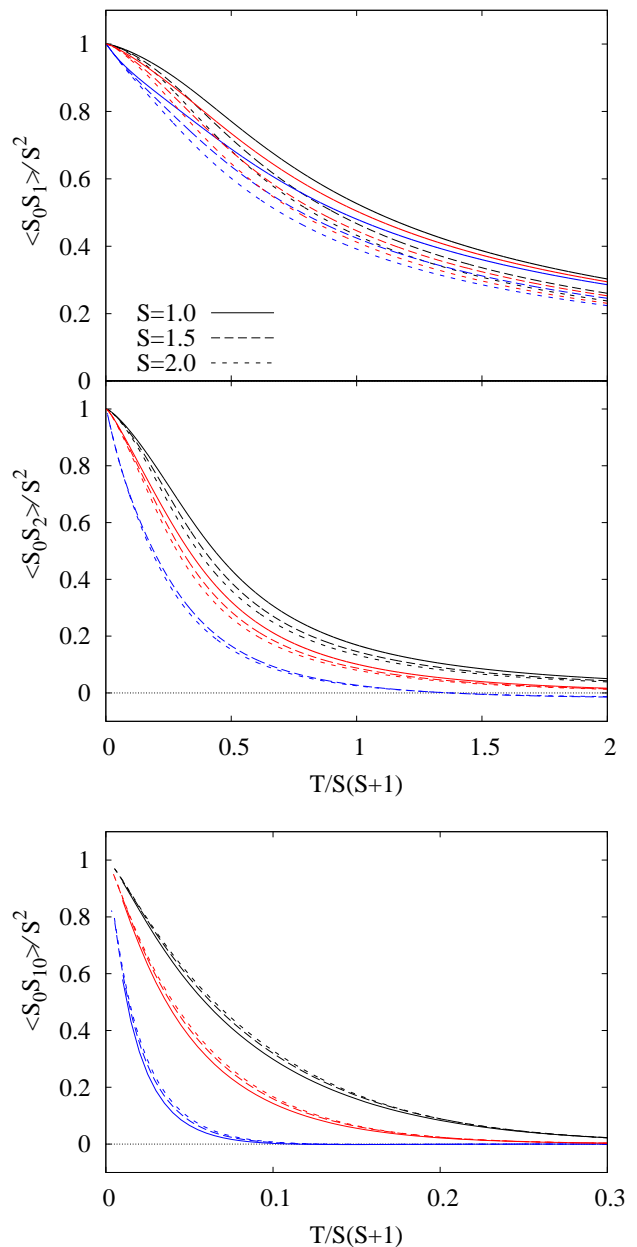


FIG. 1: Spin-spin correlation functions $\langle \mathbf{S}_0 \mathbf{S}_1 \rangle / S^2$ (NN), $\langle \mathbf{S}_0 \mathbf{S}_2 \rangle / S^2$ (NNN), and $\langle \mathbf{S}_0 \mathbf{S}_{10} \rangle / S^2$ obtained by the RGM for spin quantum numbers $S = 1$ (solid), $3/2$ (long-dashed), and $S = 2$ (short-dashed) and frustration parameters $J_2 = 0$ (black), 0.1 (red), and 0.2 (blue).

Figs. 2 and 3. We illustrate the influence of frustration for a fixed spin quantum number $S = 1$, whereas in the insets we show the influence of S for a fixed frustration parameter $J_2 = 0.1$. Since the ground state is ferromagnetic, both quantities diverge at $T = 0$. With increasing of frustration the rapid increase in χ and ξ is shifted to lower temperatures. The comparison of RGM and ED results for finite chains of $N = 12$ presented in Fig. 2

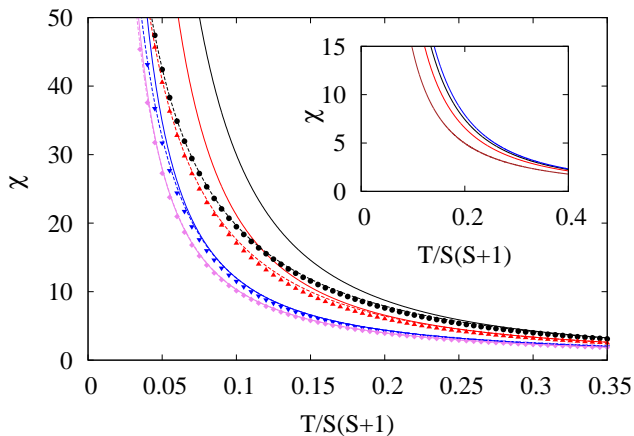


FIG. 2: Susceptibility χ for spin quantum number $S = 1$ and frustration parameters $J_2 = 0$ (black), 0.1 (red), 0.2 (blue), and 0.22 (violet) [solid lines: RGM for $N \rightarrow \infty$, dashed lines: RGM for $N = 12$, symbols: ED for $N = 12$]. Inset: Susceptibility χ for $J_2 = 0.1$ and $S = 1/2, 1, 3/2$, and 2 (from bottom to top). The data for $S = 1/2$ are taken from Ref. 7.

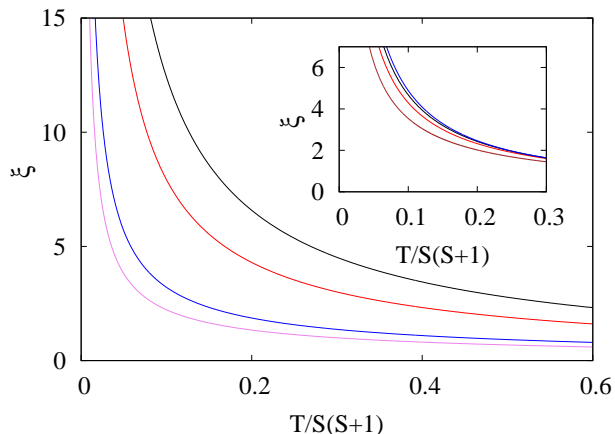


FIG. 3: Correlation length ξ for spin quantum number $S = 1$ and frustration parameters $J_2 = 0$ (black), 0.1 (red), 0.2 (blue), and 0.22 (violet). Inset: Correlation length ξ for $J_2 = 0.1$ and $S = 1/2, 1, 3/2$, and 2 (from bottom to top). The data for $S = 1/2$ are taken from Ref. 7.

demonstrates a very good agreement of the susceptibility data obtained by both methods. It can also be seen that the renormalized temperature t , where finite-size effects become relevant, is shifted to lower values of t with increasing frustration (in Fig. 2 the curves for $N = 12$ and $N \rightarrow \infty$ for $J_2 = 0.2$ and $J_2 = 0.22$ almost coincide). The curves shown in the insets again illustrate that the influence of the spin quantum number is small; only for $S = 1/2$ the curves are noticeably separated from the bundle of curves for $S > 1/2$. Moreover, it is evident that χ and ξ at fixed t and J_2 increase with growing S .

Next we consider the critical behavior of χ and ξ for

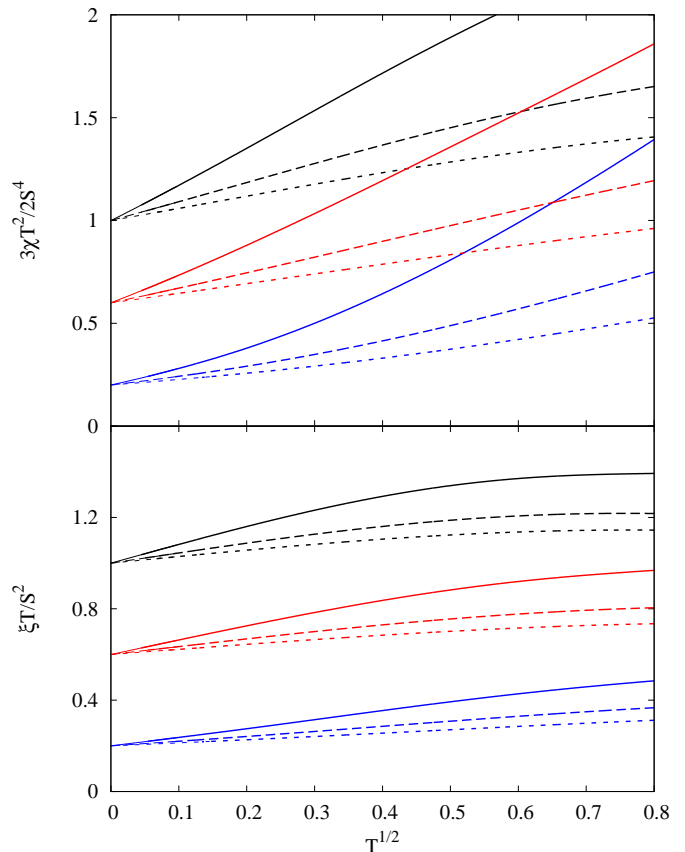


FIG. 4: RGM results for $\frac{3}{2}\chi T^2/S^4$ (upper panel) and $\xi T/S^2$ (lower panel) versus \sqrt{T} for spin quantum numbers $S = 1$ (solid), $3/2$ (long-dashed), and $S = 2$ (short-dashed) and frustration parameters $J_2 = 0$ (black), 0.1 (red), and 0.2 (blue).

$T \rightarrow 0$ by analyzing the RGM data at low temperatures. From Ref. 27 it is known that within the RGM the low-temperature behavior of χ and ξ of the unfrustrated ferromagnet ($J_2 = 0$) is given by $\lim_{T \rightarrow 0} \chi T^2 = 2S^4|J_1|/3$ and $\lim_{T \rightarrow 0} \xi T = S^2|J_1|$. These results agree with those obtained by modified spin-wave theory.^{39,40} Moreover, for $S = 1/2$ they coincide with the exact Bethe-ansatz analysis.^{40,41} (Note that χ defined in Refs. 39 and 41 is larger by a factor of four than χ given by Eq. (7).) Including higher-order terms in T for 1D Heisenberg ferromagnets the low-temperature behavior of the susceptibility and the correlation length reads $\chi T^2 = y_0 + y_1\sqrt{T} + y_2T + \mathcal{O}(T^{3/2})$ and $\xi T = x_0 + x_1\sqrt{T} + x_2T + \mathcal{O}(T^{3/2})$, see, e.g., Refs. 7,39–41. The dependence of χT^2 and ξT on $T^{1/2}$ is shown in Fig. 4 for various values of S and J_2 . The validity of linear relations $\chi T^2 \propto T^{1/2}$ and $\xi T \propto T^{1/2}$ at low temperatures is clearly seen. To determine the parameters y_0, y_1, y_2, x_0, x_1 , and x_2 , we follow the lines of Ref. 7 and fit the RGM results for χ and ξ using the relations given above. For the fits we use low-temperature data points between T_0 and $T_0 + T_{cut}$,

where T_0 is the lowest temperature for which solutions of the RGM equations can be found, see Sec. III. For T_{cut} we chose $T_{cut} = 0.005$, cf. Ref. 7. By analyzing data for $J_2 = 0$ and $S = 1, 3/2, 2$ and 5 we have numerically confirmed the relations $y_0 = 2S^4/3$ and $x_0 = S^2$ with an accuracy of at least three digits. For the next-to-leading coefficients we adopt the relations $y_1/S^4 = \alpha_0 S^{\alpha_1}$ and $x_1/S^2 = \beta_0 S^{\beta_1}$ found by modified spin-wave theory for the unfrustrated model.^{39,40} We find $\alpha_0 = 1.106$, $\alpha_1 = -1.497$, $\beta_0 = 0.834$, and $\beta_1 = -1.495$, which is in good agreement with the results of Refs. 39 and 40, where $\alpha_0 = 0.824$, $\alpha_1 = -1.5$, $\beta_0 = 0.412$, and $\beta_1 = -1.5$ were reported.

Now we determine the parameters y_0, y_1, y_2, x_0, x_1 , and x_2 for finite frustration $J_2 > 0$. The results for the leading coefficients y_0 and x_0 are shown in the insets of Fig. 5. Both coefficients y_0 and x_0 obey with high precision the linear relations $y_0/S^4 = \frac{2}{3}(|J_1| - 4J_2)$ and $x_0/S^2 = |J_1| - 4J_2$, i.e., the leading coefficients decrease with growing frustration and vanish finally at the quantum critical point $J_2^c = |J_1|/4$, thus indicating a change of the critical exponent of χ and ξ at J_2^c . This linear decrease of y_0 and x_0 found by fitting the low-temperature behavior of χ and ξ is the same as that obtained analytically for the zero-temperature spin stiffness ρ_s , see Sec. III. This correspondence between the spin stiffness and the divergence of the susceptibility and the correlation length is in accordance with general arguments^{42,43} concerning the low-temperature physics of low-dimensional Heisenberg ferromagnets. Moreover, these linear relations agree with the findings for $S = 1/2$ (Ref. 7) and $S \rightarrow \infty$ (Ref. 25).

Next we determine the coefficients y_1 and x_1 as functions of J_2 again using the fit of the RGM data for $S = 1, 3/2, 2$ and 5 described above. Moreover, we reanalyze our data for $S = 1/2$ from Ref. 7. Using an improved computer code we are able to add $S = 1/2$ data for $J_2 = 0.22$ not given in Ref. 7. Similar as for y_0/S^4 and x_0/S^2 , the data for y_1 and x_1 shown in Fig. 5 yield evidence for a universal J_2 dependence of $y_1/S^{5/2}$ and $x_1/S^{1/2}$. However, the coincidence of the data points is less pronounced (in particular for $S = 5$) than for y_0 and x_0 . The dependence of $y_1/S^{5/2}$ and $x_1/S^{1/2}$ on J_2 is clearly not linear. As suggested by the behavior of $y_1/S^{5/2}$ and $x_1/S^{1/2}$ at larger J_2 we chose $f(J_2) = a\sqrt{1 - bJ_2}$ to fit the data points presented in Fig. 5. These fits suggest, that y_1 and x_1 also vanish approaching the quantum critical point. Indeed, we find for the fit parameter $b \approx 4.08$ for most of the fits; only for $S = 1/2$ we have $b \approx 4.20$. For comparison, we also show the previous quadratic fit for $S = 1/2$ of Ref. 7, where the data point at $J_2 = 0.22$ was not included. It is obvious that the square-root fit is more reasonable than the quadratic fit (which leads to a finite y_1 and x_1 at $J_2 = |J_1|/4$). Moreover, a square-root dependence of y_1 and x_1 on the exchange couplings is also suggested by modified spin-wave theory.^{39,40,44} Based on the results for y_0, y_1, x_0 , and x_1 discussed above we finally argue that the low-temperature behavior of the sus-

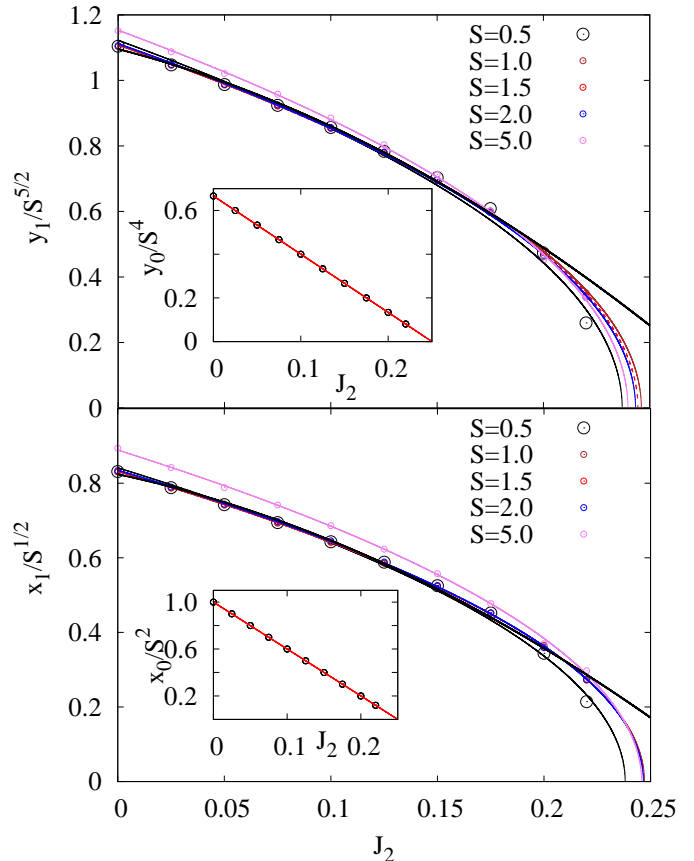


FIG. 5: Next-to-leading coefficients $y_1/S^{5/2}$ (upper panel) and $x_1/S^{1/2}$ (lower panel) in dependence on J_2 obtained by fitting the low-temperature data of χ and ξ (see main text). The symbols represent the data points for $S = 1/2, 1, 3/2, 2$, and $S = 5$, and the lines of the same color show the corresponding fit curves of these points using the fit function $f(J_2) = a\sqrt{1 - bJ_2}$. The thick black solid line shows the quadratic fit for $S = 1/2$ without the data point at $J_2 = 0.22$ as used in Ref. 7.

Insets: Leading coefficients y_0 (upper panel) and x_0 (lower panel) in dependence on J_2 obtained by fitting the low-temperature data of χ and ξ (see main text). The values for y_0/S^4 as well as for x_0/S^2 practically coincide for $S = 1/2, 1, 3/2, 2$, and $S = 5$ used to determine y_0/S^4 and x_0/S^2 .

ceptibility and the correlation length for $J_2 < |J_1|/4$ is well described by

$$\chi T^2 = \frac{2}{3}S^4 (|J_1| - 4J_2) + AS^{5/2} \sqrt{(|J_1| - 4J_2)\sqrt{T}} \quad (8)$$

and

$$\xi T = S^2 (|J_1| - 4J_2) + BS^{1/2} \sqrt{(|J_1| - 4J_2)\sqrt{T}} \quad (9)$$

with $A \approx 1.1$ ($A \approx 1.2$) and $B \approx 0.84$ ($B \approx 0.89$) for $S = 1/2, 1, 3/2$, and 2 ($S = 5$). Therefore, we conclude that, in accordance with previous results for $S = 1/2$ and

$S = \infty$, see Refs. 7 and 25, the critical behavior of χ and ξ is changed at the quantum critical point over the entire range of spin quantum numbers, $1/2 \leq S \leq \infty$. We may speculate, that the expansion $\chi T^2 = y_0 + y_1 \sqrt{T} + y_2 T + \mathcal{O}(T^{3/2})$ and $\xi T = x_0 + x_1 \sqrt{T} + x_2 T + \mathcal{O}(T^{3/2})$ valid for $J_2 < |J_1|/4$ breaks down at the quantum critical point $J_2^c = |J_1|/4$, and the critical behavior found for the classical system at J_2^c , $\chi \propto T^{-4/3}$ and $\xi \propto T^{-1/3}$, may hold also for the quantum model. However, recent numerical studies⁴⁴ indicate a slightly different critical behavior for $S = 1/2$.

C. Specific heat

Finally we discuss the specific heat C_V , see Figs. 6 and 7. With increasing of S there is a shift of the broad maxi-

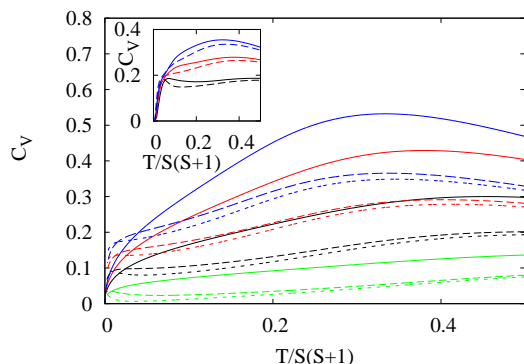


FIG. 6: Specific heat for $S = 1/2$ (green), $S = 1$ (black), $S = 3/2$ (red), and $S = 2$ (blue) obtained by RGM for $J_2 = 0$ (solid), $J_2 = 0.22$ (long-dashed), and $J_2 = 0.22$ (short-dashed). Inset: ED results for $N = 8$ and $S = 1$ (black), $3/2$ (red) and 2 (blue) for $J_2 = 0.2$ (solid) and $J_2 = 0.22$ (dashed).

imum typical for spin systems to lower values of the renormalized temperature $t = T/S(S+1)$ and an increase of its height, see Fig. 6. For fixed S the frustration J_2 leads to a decrease of this maximum. Of particular interest is the low-temperature behavior of the specific heat. In Ref. 7 an additional frustration-induced low-temperature maximum in the specific heat was found for the $S = 1/2$ model studied by RGM and ED. From Fig. 6 it is obvious that for higher values of S this additional maximum disappears. Note that this observation is similar to the findings in Ref. 21 for a field-induced low-temperature maximum in C_V , which appears for low values of S only. To be more specific, we find that for $S > 1$ no extra maximum appears in the RGM data for C_V in the whole range of $0 < J_2 \leq 0.22$ accessible within the RGM approach. The frustration-induced low-temperature maximum for $S = 1/2$ appears in the RGM for $J_2 \geq 0.16$ (Ref. 7). For $S = 1$ we find that a double-maximum structure in C_V calculated by RGM appears for $J_2 \geq 0.21$.

These RGM based results are supported by finite-size

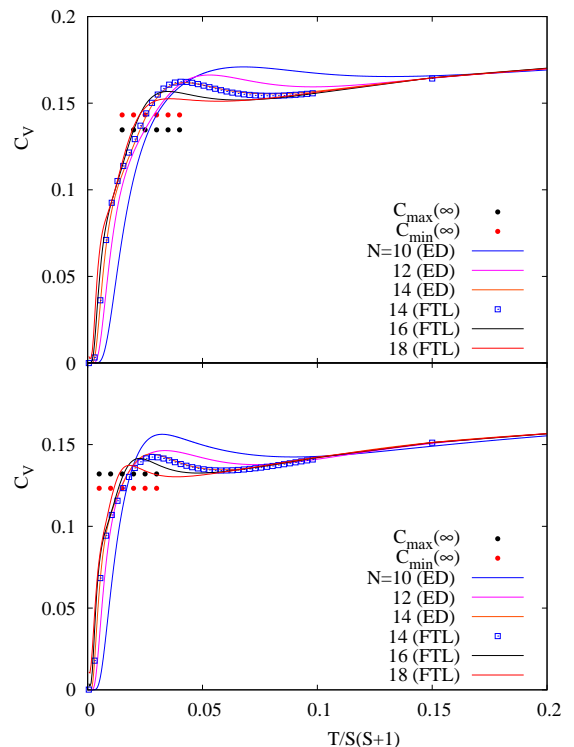


FIG. 7: Exact diagonalization (ED) and finite-temperature Lanczos (FTL) results for the low-temperature maximum in the specific heat for $S = 1$ and $J_2 = 0.2$ (upper panel) and $J_2 = 0.22$ (lower panel) for chain lengths $N = 10, 12, 14, 16$ and 18 . For $N = 14$ we present both the exact ED and the approximate FTL data to demonstrate the accuracy of the FTL technique down to very low temperatures.

data (see inset of Fig. 6), i.e. we find also in the ED data for $N = 8$ a clear tendency to suppress the extra low-temperature maximum if S increases. In more detail we analyze finite-size data for $S = 1$, where the larger systems are accessible by numerical methods. In Fig. 7 we illustrate the finite size-effects in C_V for $S = 1$ and $J_2 = 0.2$ and 0.22 . It is obvious that the extra low-temperature maximum is appreciably affected by finite-size effects. However, from Fig. 7 it is also evident that the height of the extra low-temperature maximum as well as the nearby minimum behave monotonously with N . Hence a finite-size extrapolation of the height $C_{max}(N)$ of the extra maximum and the related minimum $C_{min}(N)$ is reasonable. Analogously to Ref. 7 we find that $a(N) = a_0 + a_1/N^2 + a_2/N^4$ as a reasonable extrapolation scheme. The results of the extrapolation are shown in Fig. 7 by black [for the extrapolated value $C_{max}^{(\infty)}$] and red [for the extrapolated value of $C_{min}^{(\infty)}$] filled circles. These extrapolated data for C_{max} and C_{min} indicate, that there is most likely no extra low-temperature maximum for $J_2 = 0.2$, but such a maximum appears for $J_2 = 0.22$. Hence, the finite-size data support the RGM predictions that the double-peak

structure appears for $S = 1$ at $J_2 \geq 0.21$.

V. SUMMARY

In this paper we have studied the influence of a frustrating NNN coupling J_2 on the thermodynamics of the 1D spin- S J_1 - J_2 Heisenberg model with ferromagnetic J_1 and antiferromagnetic J_2 with $J_2 \leq |J_1|/4$. For that we have used the RGM for infinite chains and full ED as well as the FTL technique for finite chains. We find a universal dependence of the thermodynamic quantities on the renormalized temperature $t = T/S(S+1)$ at large temperatures. At low temperatures such a universal behavior is found for the critical properties of the susceptibility $\chi T^2/S^4 = (2/3)(|J_1| - 4J_2)$ and the correlation

length $\xi T/S^2 = |J_1| - 4J_2$, i.e., the critical exponents of χ and ξ for $T \rightarrow 0$ are not changed by a frustrating $J_2 < 0.25|J_1|$. However, our data suggest that at the quantum critical point $J_2 = |J_1|/4$ the critical behavior of χ and ξ is changed.

For $S = 1/2$ and $S = 1$ an additional low-temperature maximum in the specific heat C_V emerges when J_2 approaches the quantum critical point. Since we did not observe such an additional maximum in C_V for $S > 1$, it can be attributed to strong quantum fluctuations present at small values of S .

Acknowledgment: We thank the DFG for financial support (grants DR269/3-1 and RI615/16-1). Computing time at the Leibniz Computing Center in Garching is gratefully acknowledged.

-
- ¹ H.P. Bader and R. Schilling, Phys. Rev. B **19**, 3556 (1979).
² A.V. Chubukov, Phys. Rev. B **44**, 4693 (1991).
³ F. Heidrich-Meisner, A. Honecker, and T. Vekua, Phys. Rev. B **74** 020403(R) (2006).
⁴ D.V. Dmitriev, V.Ya. Krivnov, and J. Richter, Phys. Rev. B **75**, 014424 (2007).
⁵ D.V. Dmitriev and V.Ya. Krivnov, Phys. Rev. B **77**, 024401 (2008).
⁶ T. Hikihara, T. Momoi, A. Furusaki, and H. Kawamura Phys. Rev. B **78**, 144404 (2008).
⁷ M. Härtel, J. Richter, D. Ihle, and S.-L. Drechsler, Phys. Rev. B **78**, 174412 (2008); J. Richter, M. Härtel, D. Ihle, and S.-L. Drechsler, J.Phys.:Conf.Ser. **145**, 012064 (2009).
⁸ R. Zinke, S.-L. Drechsler, and J. Richter, Phys. Rev. B **79**, 094425 (2009).
⁹ J. Sudan, A. Luscher, and A. Läuchli, Phys. Rev. B **80**, 140402(R) (2009).
¹⁰ J. Sirker, Phys. Rev. B **81**, 014419 (2010).
¹¹ M. Härtel, J. Richter, and D. Ihle, arXiv:1102.3531 (accepted Phys.Rev.B).
¹² S. Nishimoto, S.-L. Drechsler, R.O. Kuzian, J. van den Brink, J. Richter, Y. Skourski, W.E.A. Lorenz, R. Klingeler, and B. Büchner, arXiv:1004.3300 (2010) and Phys. Rev. Lett. (in press).
¹³ K. Kudo, S. Kurogi, Y. Koike, T. Nishizaki, and N. Kobayashi Phys. Rev. B **71**, 104413 (2005).
¹⁴ S.-L. Drechsler, O. Volkova, A.N. Vasiliev, N. Tristan, J. Richter, M. Schmitt, H. Rosner, J. Málek, R. Klingeler, A.A. Zvyagin, and B. Büchner, Phys. Rev. Lett. **98**, 077202 (2007).
¹⁵ J. Málek, S.-L. Drechsler, U. Nitzsche, H. Rosner, and H. Eschrig, Phys. Rev. B **78**, 060508 (2008).
¹⁶ C.P. Landee and R.D. Willett, Phys. Rev. Lett. **43**, 463 (1979); C. Dupas, J.P. Renard, J. Seiden, and A. Cheikh-Rouhou, Phys. Rev. B **25**, 3261 (1982).
¹⁷ J. K. Kjems and M. Steiner, Phys. Rev. Lett. **41**, 1137 (1978); T. Delica, W.J. de Jonge, K. Kopinga, H. Leschke, and H.J. Mikeska, Phys. Rev. B **44**, 11773 (1991).
¹⁸ W. Zhang, C. P. Landee, M. M. Turnbull, and R. D. Willett, J. Appl. Phys. **73**, 5379 (1993)
¹⁹ P. Gambardella, A. Dallmeyer, K. Maiti, M.C. Malagoli, W. Eberhardt, K. Kern, and C. Carbone, Nature **416**, 301 (2002); A. Vindigni, A. Rettori, M.G. Pini, C. Carbone, and P. Gambardella, Appl. Phys. A **82**, 385 (2006).
²⁰ F.D.M. Haldane, Phys. Lett. A **93**, 464 (1983); Phys. Rev. Lett. A **50**, 1153 (1983).
²¹ I. Juhász Junger, D. Ihle, L. Bogacz, and W. Janke, Phys. Rev. B **77**, 174411 (2008).
²² I. Junger, D. Ihle, J. Richter, and A. Klümper, Phys. Rev. B **70**, 104419 (2004).
²³ T.N. Antsygina, M.I. Poltavskaya, I.I. Poltavsky, and K.A. Chishko, Phys. Rev. B **77**, 024407 (2008).
²⁴ M. Härtel, J. Richter, D. Ihle, and S.-L. Drechsler, Phys. Rev. B **81**, 174421 (2010).
²⁵ D.V. Dmitriev and V.Y. Krivnov, Phys. Rev. B **82**, 054407 (2010); arXiv:1007.4536 (unpublished)
²⁶ J. Kondo and K. Yamaji, Prog. Theor. Phys. **47**, 807 (1972); H. Shimahara and S. Takada, J. Phys. Soc. Jpn. **60**, 2394 (1991); S. Winterfeldt and D. Ihle, Pys. Rev. B **56**, 5535 (1997).
²⁷ F. Suzuki, N. Shibata, and C. Ishi, J. Phys. Soc. Jpn. **63**, 1539 (1994).
²⁸ W. Yu and S. Feng, Eur. Phys. J. B **13**, 265 (2000); L. Siurakshina, D. Ihle, and R. Hayn, Phys. Rev. B **64**, 104406 (2001); B.H. Bernhard, B. Canals, and C. Lacroix, Phys. Rev. B **66**, 024422 (2002); D. Schmalfuß, J. Richter, and D. Ihle, Phys. Rev. B **70**, 184412 (2004); D. Schmalfuß, J. Richter, and D. Ihle, Phys. Rev. B **72**, 224405 (2005); D. Schmalfuß, R. Darradi, J. Richter, J. Schulenburg, and D. Ihle, Phys. Rev. Lett. **97**, 157201 (2006).
²⁹ I. Juhász Junger, D. Ihle, and J. Richter, Phys. Rev. B **72**, 064454 (2005).
³⁰ I. Juhász Junger, D. Ihle, and J. Richter, Phys. Rev. B **80**, 064425 (2009).
³¹ J. Schulenburg, program package *spinpack*, <http://www-e.uni-magdeburg.de/jschulen/spin/>
³² W. Gasser, E. Heiner and K. Elk, *Greensche Funktionen in Festkörper- und Vielteilchenphysik* (WILEY-VCH Verlag, Berlin 2001).
³³ J. Jaklic and P. Prelovsek, Phys. Rev. B **49**, 5065 (1994); Adv. Phys. **49**, 1 (2000).
³⁴ J. Schnack and O. Wendland, Eur. Phys. J. B **78**, 535 (2010).
³⁵ H.-J. Mikeska and A.K. Kolezhuk, in *Quantum Mag-*

- netism*, eds. U. Schollwöck, J. Richter, D.J.J. Farnell, and R.F. Bishop, Eds., Lecture Notes in Physics **645** (Springer, Berlin, 2004), p. 1.
- ³⁶ T. Hamada, J. Kane, S. Nakagawa, and Y. Natsume, J. Phys. Soc. Jpn. **57**, 1891 (1988); **58**, 3869 (1989).
- ³⁷ G.S. Rushbrooke, G.A. Baker, and P.J. Wood, in *Phase Transitions and Critical Phenomena*, Vol. 3, p. 245; eds. C. Domb and M.S. Green, Academic Press, London, 1974.
- ³⁸ J. Oitmaa, C.J. Hamer, and W.H. Zheng, *Series Expansion Methods*. Cambridge University Press, 2006.
- ³⁹ M. Takahashi, Prog. Theor. Phys. Supp. **87**, 233 (1986); M. Takahashi, Phys. Rev. Lett. **58** 168 (1987).
- ⁴⁰ M. Yamada, J. Phys. Soc. Jpn. **59**, 848 (1990).
- ⁴¹ M. Yamada and M. Takahashi, J. Phys. Soc. Jpn. **55**, 2024 (1986).
- ⁴² P. Kopietz and G. Castilla, Phys. Rev. B **43** 11100 (1991).
- ⁴³ N.B. Ivanov, Condens. Matter Phys. (L'viv) **12**, 435 (2009) (see also arXiv:0909.2182).
- ⁴⁴ J. Sirker, V.Y. Krivnov, D.V. Dmitriev, A. Herzog, S. Nishimoto, S.-L. Drechsler, O. Janson, and J. Richter, in preparation.